Original Article
Food Science and Technology

ISSN 0101-2061 (Print)
ISSN 1678-457X (Online)

DOI: https://doi.org/10.1590/fst.129922

Evaluation of maturity and moisture content in fresh jujube using fractal theory and tissue images

Xueting MA[1,2], Fei ZHANG[1,2], Huaping LUO[1,2*], Feng GAO[1,2]

Abstract

This study proposes a novel method for jujube maturity and water content determination incorporating fractal theory. Firstly, the tissue section images of winter jujube at different maturity and tissue section image images of winter jujube with different moisture content were preprocessed by grayscale, median filter, histogram equalization and binarization. Secondly, the fractal dimension of jujube tissue section images of jujube at different maturity, and the fractal dimension of tissue slice images of jujube with different moisture content were calculated based on the box dimension algorithm. Finally, the relationships of the fractal dimension-maturity and fractal dimension-moisture content were explored. The results showed that the fractal features had good discrimination performance, the fractal dimension decreased with the increase of maturity, and the fractal dimension decreased with the increase of moisture content. This study provides a new way of thinking about the detection of physical and chemical indicators of winter jujube and other fruits.

Keywords: maturity; moisture content; fractal theory; tissue section image; jujube.

Practical Application: Evaluation of maturity and moisture content in fresh jujube microflora.

1 Introduction

Jujube is rich in vitamins, polysaccharides, organic acids and amino acids, etc. It has high nutritional value and medicinal value, and is one of the most popular fruits for consumers (Wang et al., 2022). The maturity and moisture content directly affect the taste and fruit quality of jujube (Fu et al., 2021; Sun et al., 2022; Wang et al., 2020), therefore, the researches on jujube maturity and moisture content detection have important significance. Many researchers have studied the detection methods of moisture content and maturity of jujube by selecting appropriate input data and building suitable predictive models.

Mahmood et al. (2022) successfully divided jujubes into three categories (unripe, ripe, and over-ripe) based on the convolutional neural network (CNN) according to maturity, which provided theoretical support for the automatic classification system of jujube. Sun et al. (2022) used the class balance loss (CB) to improve the MobileNetV2 network, and used A transfer learning strategy to train the model. The results showed that the CB-MobileNet V2 model improved the performance of jujube maturity classification. Zang et al. (2021) provided an automatic weighing method and machine vision system to detect the moisture content of jujube slices, allowing real-time detection during the drying process to come true on the strength of the LABVIEW virtual tool.

In recent years, the fractal theory has been more and more widely used in image processing. Fractal theory is an important branch of modern nonlinear science and an important mathematical tool and means in scientific research. Its research objects are irregular and self-similar geometric shapes that widely exist in nature and real life (Ma et al., 2023). Fractal theory can condense the numerous and complex texture features of image into a concise digital expression (Acquisgrana et al., 2022), that is, fractal dimension, which can reveal the hidden information of jujube quality change. The theory was proposed by Professor Mandelbrot (Mandelbrot, 1967), and is often used to process vibration signals (Huang et al., 2022) and texture features (Yao et al., 2021). Its application fields include fault diagnosis (Liang et al., 2022), tool wear detection (Zhao et al., 2021), face recognition (Tang et al., 2018), medical diagnosis (Ibrahim et al., 2022), etc.

However, there are few reports on the application of this theory in fruit quality detection. In this study, fractal theory was applied to the quality detection of fresh jujube. In view of the fact that sliced tissue images can well reflect the quality information of jujube, the tissue images of jujube were taken as the research object. Based on the fractal theory, the fractal characteristics of the data were extracted, and the relationship of fractal characteristics-moisture content and fractal characteristics-maturity were investigated. This study provides a novel idea for jujube and other fruit quality detection. The flow chart of research on maturity and moisture content detection of fresh jujube is shown in Figure 1. Through the implementation of this study, it is expected to form a new and rapid fruit detection method and reduce the detection cost.

Received 22 Dec., 2022
Accepted 30 Jan., 2023
[1] *Modern Agricultural Engineering Key Laboratory, Universities of Education, Department of Xinjiang Uygur Autonomous Region, Tarim University, Alar, China*
[2] *College of Mechanical and Electrical Engineering, Tarim University, Alar, China*
*Corresponding author: luohuaping739@163.com

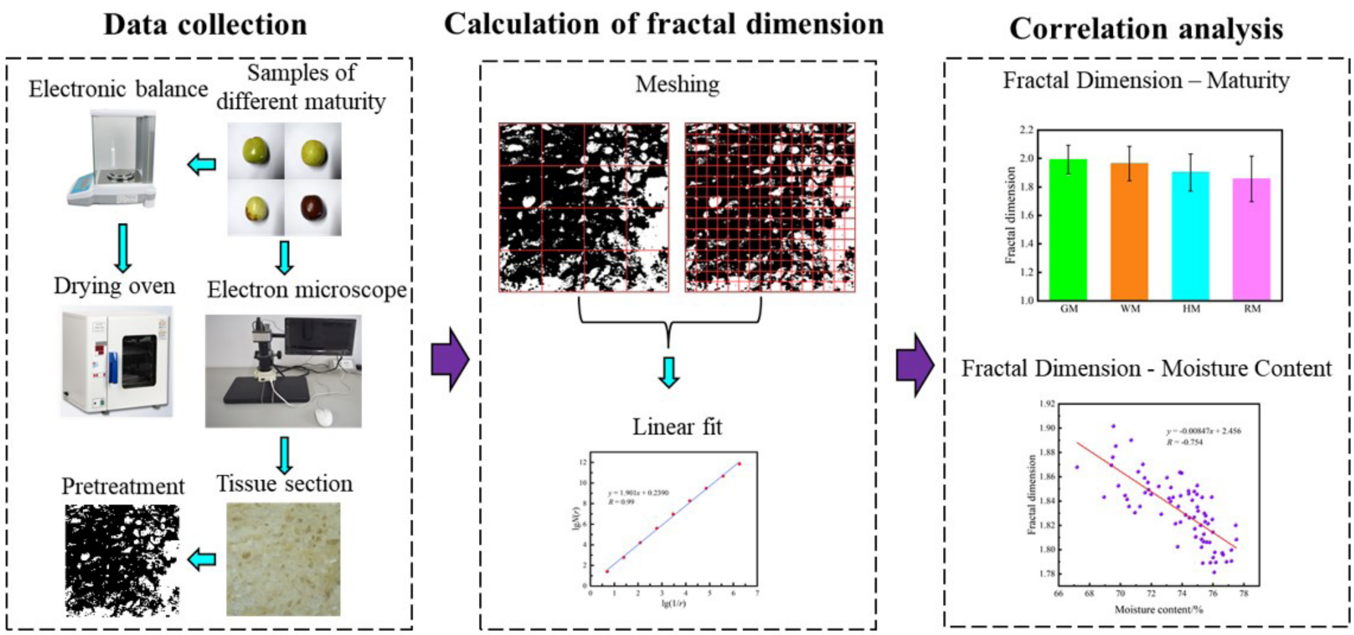

Figure 1. Flow chart of research on maturity and moisture content detection of fresh jujube.

2 Materials and methods

2.1 Sample preparation

The fresh winter jujube samples used for the experiment were picked from the jujube orchard in Alar City, Xinjiang Production and Construction Corps. Jujube samples should be free from diseases and insect pests, and be wiped to clean the surface of dust and stains after picking. We selected regular-shaped samples (longitudinal diameter (28 ± 3) mm, transverse diameter (25 ± 3) mm) and divided them into four categories according to maturity, namely green maturity (GM), white maturity (WM), half-red maturity (HM) and red maturity (RM). The images of fresh jujubes at different levels of maturity were shown in Figure 2.

2.3 Data collection

The data that needed to be obtained in this study included the moisture content of jujube and the tissue section images of jujube.

2.4 Moisture content determination

The jujube samples at red maturity (RM) were divided into 5 groups and placed in the sample trays, and stored for 24h, 48h, 72h, 96h and 120h, respectively. The moisture contents of the jujubes at different storage time were measured. The laboratory temperature was 20°C and the humidity was 20% RH.

Jujube flesh was cut to a mass of about 3 g, and the mass was measured by JA2003 electronic balance (Hunan Lichen Instrument Technology Co., Ltd.). When measuring the moisture content, the initial mass m_1 of each sample was measured first, and then the sample was put into the GZX-9140MBE electric blast drying oven (Shanghai Boxun Industrial Co., Ltd.) for drying. Then a mass measurement was carried out every 2 hours until the mass change of two adjacent measurements was less than 0.001 g, and the mass m_2 at that time was recorded. The moisture content of each sample can be calculated by Formula 1.

Figure 2. The images of fresh jujubes at different levels of maturity.

$$w = (m_1 - m_2) \cdot m_1 \times 100\% \quad (1)$$

where, w is the moisture content, m_1 is the initial mass of the sample, and m_2 is the final mass of the sample after drying.

2.5 Tissue section image acquisition

The 2 mm tissue under the epidermis at the jujube equator was taken to make jujube tissue sections. During the slicing process, the blade needs to be kept clean to avoid the influence of stains on the tissue sections. Tissue sections of jujubes at four mature stages were made and images were obtained.

TD-2KHU electron microscope (Shenzhen Sanqiang Taida Optical Instrument Co., Ltd.) was used to acquire images of jujube tissue sections. During operation, the magnification of the microscope was set to 50, and the tissue sections were photographed after adjusting the focus. Each sample was photographed 3 times, and the clearest image was selected as the test data.

2.6 Tissue section image preprocessing

To make the tissue section image better characterize the microscopic tissue state of the sample, grayscale, histogram equalization, median filter, threshold selection and binarization were successively performed on it. To improve the calculation efficiency, Matlab2021b (Mathworks, Natick, MA) software was used for data calculating, and Origin2021 (OriginLab Corporation, Northhampton, MA, USA) and Matlab2021b software were used for figure drawing.

2.7 Gray processing

A true-color image can be converted to grayscale via gray processing. Gray processing includes the component method, maximum value method, mean method and weighted mean method (Zhao et al., 2023a, b). In this study, the weighted average method was used to convert the RGB value into a gray value by weighting the three components of RGB with different weights (Figure 3). The grayscale value can be calculated by Formula 2.

$$Y = 0.299 \times R + 0.587 \times G + 0.114 \times B \tag{2}$$

2.8 Histogram equalization processing

Histogram equalization is to properly homogenize the original gray probability density distribution of the original image, and obtain a new image. Images that are too dark and too bright will become clear after histogram equalization, with rich details, which is conducive to subsequent processing (Rahman & Paul, 2023; Sule & Ezugwu, 2023). The images of histogram equalization processing of jujube tissue section were shown in Figure 4.

2.9 Median filtering processing

The function of median filtering is to calculate the median value of pixel values of the points around any point on the image, and replace the point with the calculated median value. Median filtering can reduce abnormal noise points. The algorithm is simple, and the operation process is convenient, which is widely used in image processing (Alqahtani et al., 2023; Sait & Ishak, 2023). The image of the tissue section after median filtering was shown in Figure 5.

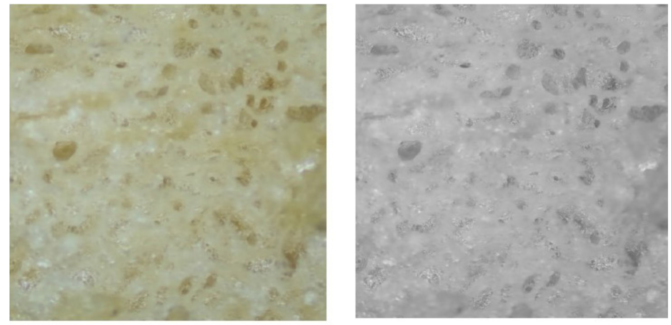

(a) The original image (b) Grayscale image

Figure 3. Gray processing of jujube tissue section image.

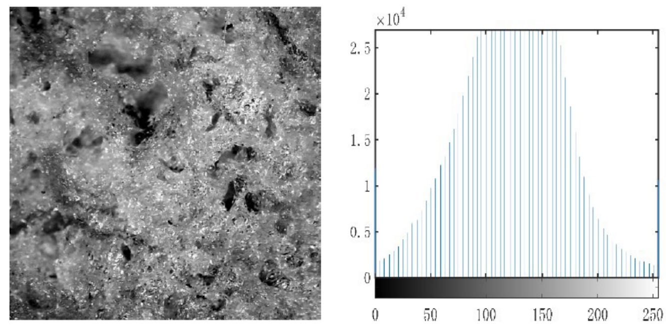

(a) Tissue section image after histogram equalization (b) Histogram of tissue section after histogram equalization

Figure 4. Histogram equalization processing of jujube tissue section image.

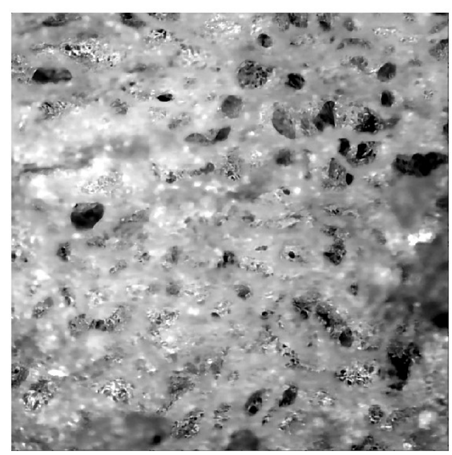

Figure 5. The image of jujube tissue section after median filtering.

2.10 Binarization processing

Image binarization is to set the gray value of the pixels on the image to 0 or 255, that is, to present the entire image with an obvious black-and-white color. Through binarization processing, the image becomes simple, the amount of data is reduced, and the target of interest can be highlighted (Li et al., 2023). The binarization process requires threshold setting. In this study, we searched for an appropriate threshold based on the maximum between-class variance method (also known as the global OTSU algorithm), which can better display the image details, and divide the picture into background and target according to the gray value of the image (Abdullah et al., 2021; Long et al., 2021). The image was represented by 1 and 0 after binarization processing. 1 was a white area, and 0 was a black area. In this study, we used white to represent the color of the pore in the jujube tissue, so it was necessary to have negative binarization processing after binarization. The binarization and negative binarization of the tissue section image were shown in Figure 6.

2.11 Fractal dimension calculation

The calculation methods of fractal dimension include correlation dimension (Zhang et al., 2021), information dimension (Qiang et al., 2022), box dimension (Xiao, 2022) and so on. Among them, the box dimension is widely used because of its simple calculation process and easy operation. The fractal dimension of jujube tissue section images was calculated based on this algorithm in this study.

The process of the box dimension calculation is: (1) the small boxes with side length r_1 are used to cover the entire image, and the number of boxes containing target information $N(r_1)$ is counted, and then the side length r_1 of the small box and the number $N(r_1)$ of small boxes are recorded; (2) the side length of the small boxes are changed to r_2, and the above step repeated, and then the side length r_2 of the small box and the number $N(r_2)$ of small boxes are recorded; (3) the side length of the small boxes continues to change, and finally, multiple sets of data are obtained (Figure 7); (4) a lg(1/r) - lg(N(r)) scatter diagram is plotted according to the recorded data, and performed linear fitting based on the least square method, then the slope k of the fitted line is the box dimension D of the jujube tissue section image (Figure 8). The box dimension of each image can be calculated by Formula 4.

$$lg\left(N(r)\right) = D \cdot lg\left(1/r\right) \quad (4)$$

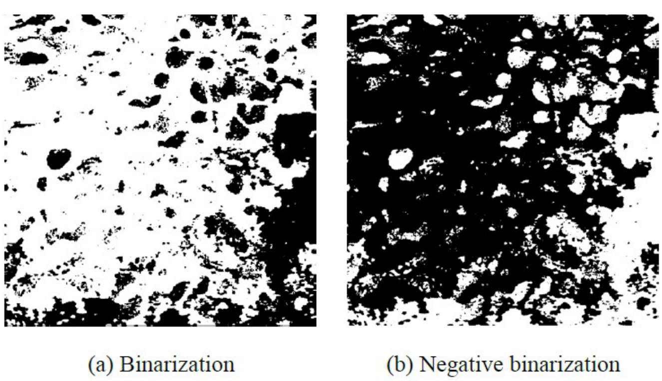

Figure 6. Binarization and negative binarization of tissue section image.

3 Results and discussion

3.1 Relationship between jujube maturity and fractal dimension

As shown in Figure 9, Figure 10, Figure 11, Figure 12 and Figure 13, the fractal characteristics of jujube tissues at different maturity stages were different. As shown in Table 1 and Figure 13, with the increase of maturity, the fractal dimension of internal tissue images of jujube gradually decreased. Among them, the mean fractal dimension of the jujube at green maturity (GM) was 1.9921, the mean fractal dimension of the jujube at white maturity (WM) was 1.9637, the mean fractal dimension of the jujube at half-red maturity (HM) was 1.9019, and the mean fractal dimension of the jujube at red maturity (RM) was 1.8556.

The internal tissue of jujube was constantly developing and growing with the increase of maturity of jujube. We could find that the tissue at green maturity was closely arranged by electron microscope, and the white part almost filled the whole area after preprocessing. As shown in Table 1, the fractal dimension obtained at that time was 1.9921, which was close to 2. As the maturity of jujube increased, the internal tissue of jujube expanded, and the white part gradually decreased after tissue section pretreatment, and the calculated fractal dimension

Table 1. Statistics of fractal dimension of jujube at different maturity.

Maturity	GM	WM	HM	RM
Mean fractal dimension	1.9921	1.9637	1.9019	1.8556

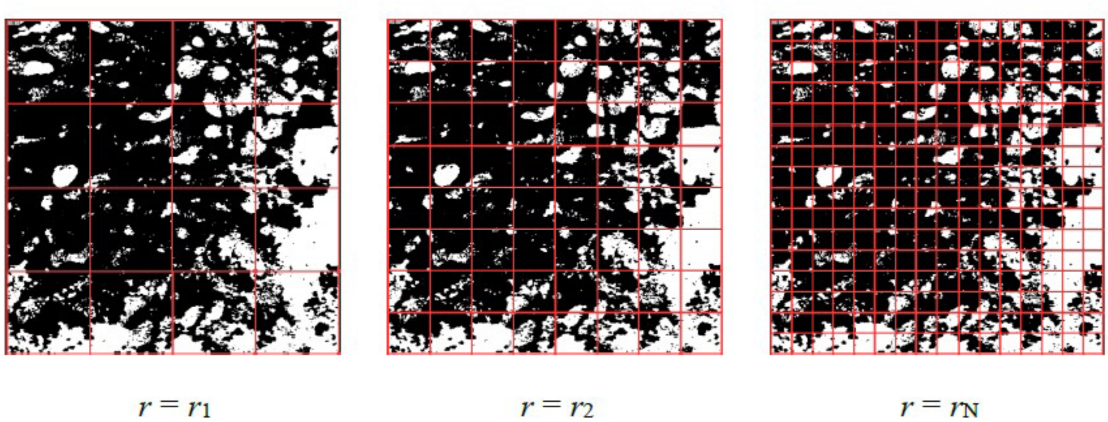

Figure 7. Image division based on box dimension algorithm.

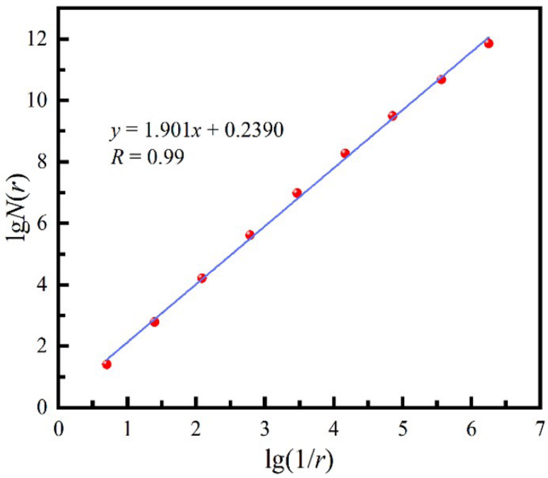

Figure 8. Linear fitting processing of scatter plot.

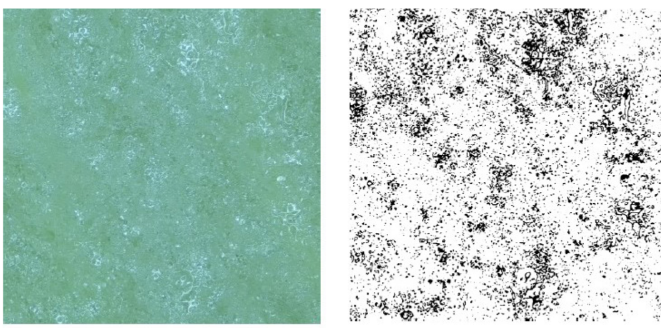

(a) Original image (b) Preprocessed image

Figure 9. Tissue section images of jujube at green maturity.

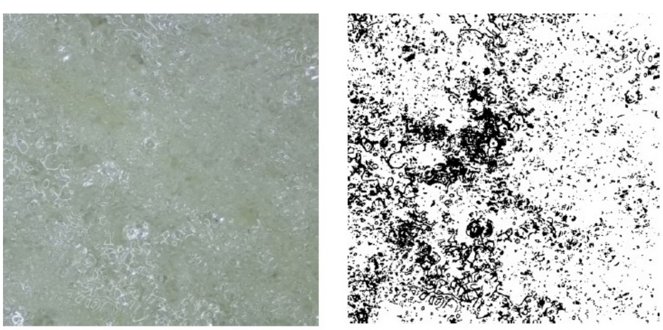

(a) Original image (b) Preprocessed image

Figure 10. Tissue section images of jujube at white maturity.

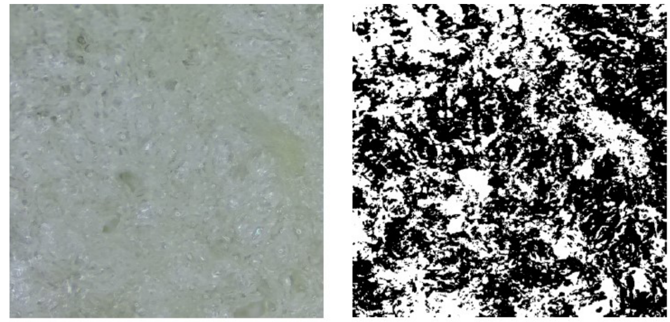

(a) Original image (b) Preprocessed image

Figure 11. Tissue section images of jujube at half-red maturity.

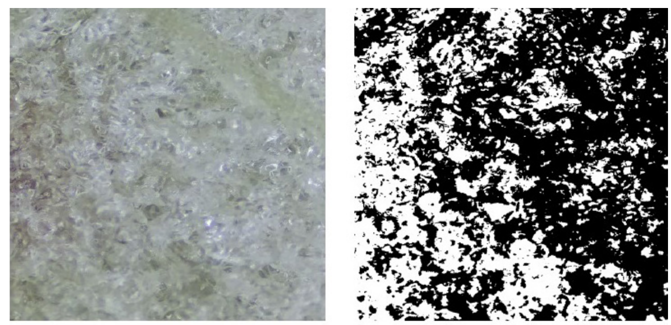

(a) Original image (b) Preprocessed image

Figure 12. Tissue section images of jujube at red maturity.

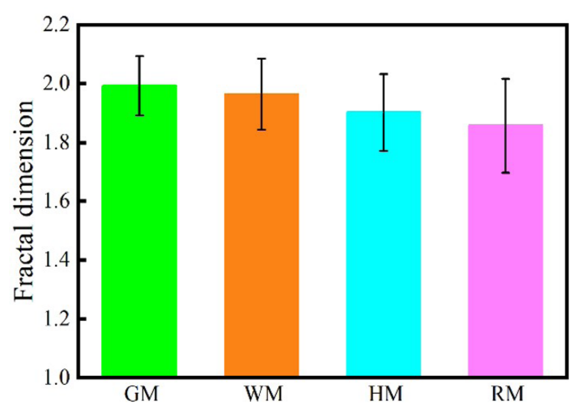

Figure 13. Fractal dimensions of jujube tissues with different maturity. Note: GM means green maturity, WM means white maturity, HM means half-red maturity, and RM means red maturity.

gradually decreased. This might be because, as jujube matures, the number of pores between internal tissues decreased, which reduced the complexity of the edge of the pore outline, and finally the calculated fractal dimension was reduced.

3.2 Relationship between jujube moisture content and fractal dimension

The correlation analysis was carried out on the calculated fractal dimension and moisture content of jujube at different storage time. As shown in Figure 14, the least squares method was used for linear fitting of the scatterplot of the relationship between moisture content and fractal dimension. The fitted expression was $y = -0.847x + 2.456$, and the correlation coefficient $R = -0.754$. The relationship between the moisture content and the fractal dimension was obvious, and the fractal dimension of the tissue section was negatively correlated with the moisture content. As the moisture content increases, the fractal dimension decreased gradually, indicating that the more moisture content in the tissue section, the less complex the image. Moisture prediction could be carried out by observing

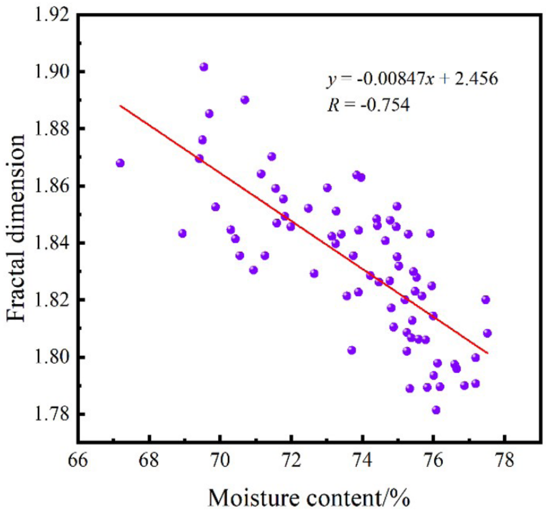

Figure 14. Scatter diagram and linear fitting of the relationship between moisture content and fractal dimension of jujube.

the microscopic images of jujube tissues. It could also be seen from Figure 14 that the fractal dimension had a good effect on the qualitative analysis of moisture content, but it was difficult to achieve accurate quantitative measurements.

4 Conclusion

In this study, the tissue section images of winter jujube were taken as the research object, and the relationship of image fractal features-jujube moisture content and fractal features-jujube maturity were explored based on fractal theory. The fractal dimensions of tissue section images with different maturity and different moisture contents were calculated based on the box dimension algorithm. Through the analysis, we found that: (1) the fractal dimension of tissue section images at different maturity levels was different, and the fractal dimension decreased gradually with the increase of maturity; (2) the fractal dimension of tissue section images with different moisture contents was different, and the fractal dimension decreased gradually with the increase of moisture content. The integration of fractal theory provides a novel idea for the detection of physical and chemical indicators of jujube and other fruits.

Ethical approval

This article does not contain any studies with human participants or animals performed by any of the authors.

Conflict of interest

The authors declare no competing interests.

Availability of data and material

All data are available from the corresponding author.

Funding

This project was supported by the National Natural Science Foundation of China (11964030) and the Open Project of Key Laboratory of Modern Agricultural Engineering in Colleges and Universities of the Department of Education of the Autonomous Region (TDNG2021201).

References

Abdullah, S., Ismail, S. M., Hasan, M. K., & Shivakumara, P. (2021). Novel Adaptive binarization method for degraded document images. *Computers Materials & Continua*, 67(3), 3815-3832. http://dx.doi.org/10.32604/cmc.2021.014610.

Acquisgrana, M. R., Gomez Pamies, L. C., Quiroga, F., Ribotta, P. D., & Benítez, E. I. (2022). Impact of sorghum grain processing on morphological characteristics of particles of wholegrain sorghum flour. *Food Science and Technology (Campinas)*, 42, 2022. http://dx.doi.org/10.1590/fst.69420.

Alqahtani, M. M., Dutta, A. K., Almotairi, S., Ilayaraja, M., Albraikan, A. A., Al-Wesabi, F. N., & Al Duhayyim, M. (2023). Sailfish optimizer with EfficientNet model for apple leaf disease detection. *Cmc-Computers Materials & Continua*, 74(1), 217-233. http://dx.doi.org/10.32604/cmc.2023.025280.

Fu, L., Yang, J., Shang, H., & Song, J. (2021). Changes of characteristic sugar, fatty acid, organic acid and amino acid in jujubes at different dry mature stages. *Journal of Food Composition and Analysis*, 104, 104. http://dx.doi.org/10.1016/j.jfca.2021.104104.

Huang, M., Wan, Z., Cheng, X., Xu, Z., Lei, Y., & Pan, D. (2022). Two-stage damage identification method based on fractal theory and whale optimization algorithm. *Advances in Structural Engineering*, 25(11), 2364-2381. http://dx.doi.org/10.1177/13694332221095629.

Ibrahim, R. W., Yahya, H., Mohammed, A. J., Al-Saidi, N. M. G., & Baleanu, D. (2022). Mathematical design enhancing medical images formulated by a fractal flame operator. *Intelligent Automation and Soft Computing*, 32(2), 937-950. http://dx.doi.org/10.32604/iasc.2022.021954.

Li, Y. F., Geng, T., Stein, S., Li, A., & Yu, H. M. (2023). GAAF: searching activation functions for binary neural networks through genetic algorithm. *Tsinghua Science and Technology*, 28(1), 207-220. http://dx.doi.org/10.26599/TST.2021.9010084.

Liang, X., Luo, Y., Deng, F., & Li, Y. (2022). Investigation on vibration signal characteristics in a centrifugal pump using EMD-LS-MFDFA. *Processes (Basel, Switzerland)*, 10(6), 1169. http://dx.doi.org/10.3390/pr10061169.

Long, J., Yan, Z., Chen, H., & Song, X. (2021). Spectrum decomposition in Gaussian scale space for uneven illumination image binarization. *PLoS One*, 16(4), e0251014. http://dx.doi.org/10.1371/journal.pone.0251014. PMid:33930072.

Ma, X. T., Luo, H. P., Liao, J. A., Zhu, L. X., Zhao, J. F., & Gao, F. (2023). Study on the detection of apple soluble solids based on fractal theory and hyperspectral imaging technology. *Food Science and Technology (Campinas)*, 43, 43. http://dx.doi.org/10.1590/fst.96722.

Mahmood, A., Singh, S. K., & Tiwari, A. K. (2022). Pre-trained deep learning-based classification of jujube fruits according to their maturity level. *Neural Computing & Applications*, 34(16), 13925-13935. http://dx.doi.org/10.1007/s00521-022-07213-5.

Mandelbrot, B. (1967). How long is the coast of Britain? Statistical self-similarity and fractional dimension. *Science*, 156(3775), 636-638. http://dx.doi.org/10.1126/science.156.3775.636. PMid:17837158.

Qiang, C. H., Deng, Y., & Cheong, K. H. (2022). Information fractal dimension of mass function. *Fractals-Complex Geometry Patterns and Scaling in Nature and Society*, 30(6), 2250110.

Rahman, H., & Paul, G. C. (2023). Tripartite sub-image histogram equalization for slightly low contrast gray-tone image enhancement. *Pattern Recognition*, 134, 134. http://dx.doi.org/10.1016/j.patcog.2022.109043.

Sait, A. R. W., & Ishak, M. K. (2023). A novel handcrafted with deep features based brain tumor diagnosis model. *Intelligent Automation and Soft Computing*, 35(2), 2057-2070. http://dx.doi.org/10.32604/iasc.2023.029602.

Sule, O. O., & Ezugwu, A. E. (2023). A two-stage histogram equalization enhancement scheme for feature preservation in retinal fundus images. *Biomedical Signal Processing and Control*, 80, 80. http://dx.doi.org/10.1016/j.bspc.2022.104384.

Sun, H. X., Zhang, S. J., Ren, R., & Su, L. Y. (2022). Maturity classification of "Hupingzao" jujubes with an imbalanced dataset based on improved mobileNet V2. *Agriculture*, 12(9), 1305. https://doi.org/10.3390/agriculture12091305.

Tang, Z., Wu, X., Fu, B., Chen, W., & Feng, H. (2018). Fast face recognition based on fractal theory. *Applied Mathematics and Computation*, 321, 721-730. http://dx.doi.org/10.1016/j.amc.2017.11.017.

Wang, N., Yu, Q. Y., Wang, D. L., Ren, H. T., Xu, C., Ning, C. C., Li, N., Fan, H. P., & Ai, Z. L. (2022). Synergistic antiaging effects of jujube polysaccharide and flavonoid in D-Galactose-Induced aging mice. *Food Science and Technology (Campinas)*, 42, 2022. http://dx.doi.org/10.1590/fst.46222.

Wang, W.-x., Ma, B.-x., Luo, X.-z., Li, X.-x., Lei, S.-y., Li, Y.-j., & Sun, J.-t. (2020). Study on the moisture content of dried hami big jujubes by near-infrared spectroscopy combined with variable preferred and GA-ELM Model. *Guangpuxue Yu Guangpu Fenxi*, 40(2), 543-549.

Xiao, W. (2022). Cardinality and fractal linear subspace about fractal functions. *Fractals-Complex Geometry Patterns and Scaling in Nature and Society*, 30(7), 2250146. https://doi.org/10.1142/S0218348X22501468.

Yao, X., Wu, Q., Zhang, P., & Bao, F. (2021). Weighted adaptive image super-resolution scheme based on local fractal feature and image roughness. *IEEE Transactions on Multimedia*, 23, 1426-1441. http://dx.doi.org/10.1109/TMM.2020.2997126.

Zang, Y. Z., Yao, X. D., Cao, Y. X., Niu, Y. B., Liu, H., Xiao, H. W., Zheng, X., Wang, Q., & Zhu, R. G. (2021). Real-time detection system for moisture content and color change in jujube slices during drying process. *Journal of Food Processing and Preservation*, 45(6). http://dx.doi.org/10.1111/jfpp.15539.

Zhang, S., Lan, W., Dai, W., Wu, F., & Chen, C. (2021). An extended correlation dimension of complex networks. *Entropy (Basel, Switzerland)*, 23(6), 710. http://dx.doi.org/10.3390/e23060710. PMid:34205073.

Zhao, J., Lin, M., Song, X., & Wei, N. (2021). A modeling method for predicting the precision loss of the preload double-nut ball screw induced by raceway wear based on fractal theory. *Wear*, 486-487, 204065. http://dx.doi.org/10.1016/j.wear.2021.204065.

Zhao, G., Liu, S., Li, G., Fang, W., Liao, Y., Li, R., Fu, L., & Wang, J. (2023a). A customizable automated container-free multi-strip detection and line recognition system for colorimetric analysis with lateral flow immunoassay for lean meat powder based on machine vision and smartphone. *Talanta*, 253, 123925. http://dx.doi.org/10.1016/j.talanta.2022.123925. PMid:36108516.

Zhao, S., Wang, P., Heidari, A. A., Zhao, X., & Chen, H. (2023b). Boosted crow search algorithm for handling multi-threshold image problems with application to X-ray images of COVID-19. *Expert Systems with Applications*, 213, 119095. http://dx.doi.org/10.1016/j.eswa.2022.119095. PMid:36313263.